Folia Microbiologica
https://doi.org/10.1007/s12223-025-01319-8

ORIGINAL ARTICLE

# Flurbiprofen restores rifampicin and isoniazid sensitivity in multidrug-resistant *Mycobacterium tuberculosis* putatively by inhibiting efflux pumps Rv0194 and Rv0933

**Padmasini Elango[1,3] · Christy Rosaline Nirmal[1,4] · Sam Ebenezer Rajadas[1,5] · Rajkumar Ravi[1] · Naresh Babu Chilamakuru[2] · Azger Dusthackeer V. N.[1]**

Received: 28 March 2025 / Accepted: 7 August 2025


**Asbtract**
Multidrug-resistant tuberculosis remains a global health challenge, necessitating novel therapeutic approaches. Efflux pumps, including Rv0194 and Rv0933, contribute to *Mycobacterium tuberculosis* resistance by actively extruding first-line drugs such as rifampicin and isoniazid. This study aimed to identify small-molecule inhibitors that target these pumps to restore drug susceptibility. Through in silico screening, six lead compounds were selected and evaluated for antimicrobial activity against ten MDR-TB clinical isolates. Among them, flurbiprofen and trichlorocarbinalide exhibited significant inhibitory effects, enhancing rifampicin and isoniazid activity in checkerboard synergy assays. These combinations reduced the minimum inhibitory concentrations of both drugs, confirming their potential to reverse resistance. Cytotoxicity assessments of peripheral blood mononuclear and THP-1 cells demonstrated favourable safety profiles. Mechanistic studies revealed increased expression of Rv0194 and Rv0933 upon rifampicin and isoniazid exposure, underscoring their role in drug resistance. Flurbiprofen and trichlorocarbinalide may enhance intracellular drug retention by inhibiting these efflux pumps, improving therapeutic efficacy. However, trichlorocarbinalide did not restore rifampicin or isoniazid sensitivity as efficiently as flurbiprofen did. These findings highlight flurbiprofen as a promising efflux pump inhibitor that could potentiate standard TB treatments and counteract resistance. Further studies using diverse clinical isolates and in vivo models are needed to validate its therapeutic potential.

**Keywords** Multidrug-resistant tuberculosis · Efflux pump inhibitors · Flurbiprofen · Rv0194 · Rv0933 · Drug synergy

## Introduction

Tuberculosis (TB) continues to be a formidable global health challenge, with an estimated 10 million new cases and 1.4 million deaths reported every year (Global Tuberculosis Programme 2023). The emergence of multidrug-resistant (MDR) and extensively drug-resistant (XDR) strains of *Mycobacterium tuberculosis* has exacerbated this situation, rendering conventional treatment regimens increasingly ineffective. MDR-TB, defined as resistance to at least isoniazid (INH) and rifampicin (RMP), and XDR-TB, which includes additional resistance to fluoroquinolones and second-line injectable drugs, pose significant challenges to global TB control efforts. The treatment of drug-resistant tuberculosis (DR-TB), although recently revised to a shorter regimen, remains expensive and is often associated with severe side effects, resulting in poor patient outcomes and high mortality rates (Davies and Aston 2023).

✉ Azger Dusthackeer V. N.
azgerdusthackeer.vn@icmr.gov.in

1 Department of Bacteriology, ICMR-National Institute for Research in Tuberculosis, No.1, Mayor Sathyamoorthy Salai, Chetpet, Chennai 600031, India

2 Department of Pharmaceutical Chemistry, Raghavendra Institute of Pharmaceutical Education and Research (RIPER)-Autonomous, K.R.Palli Cross, Anantapur 515721, India

3 Present Address: Department of Molecular Analytics, SIMATS Engineering, Saveetha University, Chennai, India

4 Present Address: Achira Labs Pvt. Ltd., No. 66B, 13th Cross, Dollar Layout, JP Nagar III Phase, Bangalore, Karnataka, India

5 Present Address: Centre for Drug Discovery and Development, Sathyabama Institute of Science and Technology, Chennai 600119, India

Published online: 22 September 2025

The development of drug resistance in *M. tuberculosis* is a complex phenomenon driven by multiple mechanisms, including genetic mutations, drug target modifications, and the activation of efflux pumps (EPs) (Remm et al. 2022). Among these, EPs play pivotal roles in mediating intrinsic and acquired resistance by actively expelling antimicrobial agents from bacterial cells, thereby reducing intracellular drug concentrations to sublethal levels (Li et al. 2015). EPs are membrane-associated transport proteins that belong to several superfamilies, including the ATP-binding cassette superfamily, the major facilitator superfamily, the multidrug and toxic compound extrusion family, the small multidrug resistance family, and the resistance−nodulation−cell−division superfamily (Guan 2022). These pumps extrude a wide range of antibiotic compounds, contributing to MDR phenotypes.

Given the critical role of EPs in drug resistance, the development of EP inhibitors (EPIs) has emerged as a promising strategy to restore drug susceptibility in resistant strains of *M. tuberculosis*. EPIs block EPs, thereby increasing the intracellular concentration of antimicrobial agents and enhancing their efficacy (Pule et al. 2016). Several classes of EPIs, including phenothiazines, verapamil, and natural compounds such as reserpine and piperine, have shown potential for reversing drug resistance in *M. tuberculosis* (de Souza et al. 2020). However, the clinical application of EPIs is limited by their toxicity, poor pharmacokinetics, and lack of specificity (Duffey et al. 2024). Therefore, the identification and development of novel EPIs with improved efficacy and safety profiles are urgently needed.

The EPs Rv0194, an ATP-binding cassette transporter, and Rv0933, a member of the major facilitator superfamily, have been identified as key players in drug resistance and are noted to be upregulated in response to antimicrobial stress, facilitating the efflux of drugs such as INH and RMP. Studies have shown that the overexpression of these EPs is associated with reduced drug susceptibility in clinical isolates of *M. tuberculosis*. For example, Rv0194 was found to be significantly induced in RMP-resistant isolates under RMP stress, highlighting its role in mediating resistance. Similarly, Rv0933 has been implicated in the efflux of multiple drugs, including INH, thereby contributing to the MDR phenotype (Long et al. 2024; Biswas and Roy 2024).

Recent studies have provided valuable insights into the structural and functional characteristics of EPs in *M. tuberculosis*. For example, structural biology approaches, including X-ray crystallography and cryo-electron microscopy, have elucidated the molecular mechanisms underlying EP function and substrate recognition. Additionally, high-throughput screening (HTS) and computational modelling have facilitated the identification of potential target-specific genes. These advances have paved the way for the rational design of novel therapeutic agents that can effectively inhibit EP activity and overcome drug resistance (Valıyeva et al. 2023). EPs, particularly Rv0194 and Rv0933, represent promising targets for the development of adjunctive therapies that can enhance the efficacy of existing anti-TB drugs. By elucidating the mechanistic roles of the identified potent EPIs Rv0194 and Rv0933, this study aims to contribute to global efforts to overcome DR-TB and achieve the WHO goal of TB eradication. Addressing efflux-mediated resistance is critical not only for improving treatment outcomes but also for reducing the transmission of drug-resistant strains, thereby mitigating the global burden of TB.

## Materials and methods

### In silico screening of EPIs against Rv0933 and Rv0194

The three-dimensional (3D) structures of the efflux pump proteins Rv0933 and Rv0194 were predicted via I-TASSER (Iterative Threading ASSEmbly Refinement), a comprehensive and widely used protein structure prediction tool. I-TASSER employs a hierarchical approach that combines multiple threading alignments and iterative structural assembly simulations to generate accurate models of protein structures (Zhang 2008). The amino acid sequences of Rv0933 and Rv0194 were retrieved from the *M. tuberculosis* genome database and submitted to the I-TASSER server. The server generated a series of structural models, from which the best model was selected on the basis of the C score, a confidence score estimating the quality of the predicted structures. The predicted 3D structures of Rv0933 and Rv0194 were further analysed to identify potential active sites via the online tool SCFBio IIT Delhi to determine the functional regions of these efflux pumps.

### Ramachandran plot analysis

The structural and stereochemical properties of the predicted protein models were assessed via Ramachandran plots. The overall geometry of the models was analysed via the PROCHECK tool, which examines residue-by-residue geometry to determine the stereochemical quality of each predicted structure. The accuracy of the predicted protein structures was further validated via the PDBsum server to generate Ramachandran plots. In these plots, the core regions indicated conformations without steric hindrance; allowed regions represented conformations possible with slightly shorter van der Waals radii (allowing atoms to come closer together), and the white areas denoted sterically unfavourable conformations.

## In silico docking studies

The predicted structures of Rv0933 and Rv0194 were individually docked against known efflux pump inhibitors, such as verapamil, thioridazine, and chlorpromazine. Molecular docking was performed via AutoDock Vina, a widely used docking software that predicts the binding affinity and mode of interactions between proteins and ligands (Morris et al. 2009). The docking results provide insights into the binding interactions of these compounds and their potential inhibitory effects on efflux pumps.

## Pharmacophore-based virtual screening

E-pharmacophore models were generated for RMP and INH on the basis of their interactions with the predicted structures of Rv0933 and Rv0194 to determine the spatial arrangement of features essential for a molecule's biological activity. The e-pharmacophore models were ranked and scored on the basis of their fit to known inhibitors. The top three highly scored models were selected for further analysis to identify energetically favourable sites on the protein that interact specifically with the ligands, thereby guiding the design of new inhibitors (Shelley et al. 2007).

The validated pharmacophore models were used as 3D queries to search against the ZINC database. The ZINC database is a comprehensive collection of commercially available compounds for virtual screening (Irwin and Shoichet 2005). The screening process identified compounds that matched the pharmacophore model and had the potential to inhibit Rv0933 and Rv0194. The hits from the virtual screening were ranked on the basis of their fitness scores, and compounds with fitness scores above 1.0 were selected for further studies.

The stability of the shortlisted lead compounds in complex with the EP proteins was assessed by calculating the binding free energy via molecular dynamics simulations. The binding free energy was calculated via tools such as MM-PBSA (molecular mechanics Poisson−Boltzmann surface area), which provides an estimate of the free energy of binding between the protein and ligand (Kollman et al. 2000). Lead compounds with binding free energy scores greater than − 80 kcal/mol were considered for further evaluation.

## ADMET property prediction

The selected lead compounds were subjected to ADMET (absorption, distribution, metabolism, excretion, and toxicity) property prediction to assess their drug-likeness and potential for human use. ADMET prediction includes evaluations of human intestinal absorption, hepatotoxicity, blood−brain barrier penetration, and compliance with Lipinski's rule of five, which predicts the oral bioavailability of compounds (Lipinski et al. 2001). Tools such as ADMET Predictor or online platforms such as pkCSM were used for this analysis (Pires et al. 2015). Only compounds with favourable ADMET properties were considered for further development as potential therapeutics against MDR and XDR strains of *M. tuberculosis*.

## Determination of MICs against MDR-TB clinical isolates

The minimum inhibitory concentrations (MICs) of the selected potential EPIs were determined against MDR-TB clinical isolates and the reference strain *M. tuberculosis* H37Rv as described previously (Nirmal et al. 2023a). In brief, the bacterial cultures of H37Rv and MDR-TB isolates grown on Lowenstein–Jensen (LJ) media were scraped carefully without disturbing the media, and the culture suspensions were prepared in Biju bottles. This suspension was adjusted to match the McFarland standard 1.0 and further diluted at a 1:10 ratio with the Middlebrook 7H9 broth supplemented with OADC and Tween 80 to achieve the desired inoculum size. Stock solutions of the lead molecules were prepared in DMSO and serially diluted in 7H9 broth to achieve a concentration range of 250–2500 µg/mL. Twofold serial dilutions were prepared in a 96-well microtiter plate, and an equal volume of bacterial suspension was added to each well, resulting in the final desired concentration range. Positive and negative controls were included to validate the growth conditions and medium sterility. The plates were incubated at 37 °C for 4 days or until growth occurred on the culture control plates. Bacterial growth, indicated by cord formation, was visually assessed using an inverted microscope. The MIC was defined as the lowest concentration of the lead molecule that completely inhibited visible growth. The assay was performed in triplicate, and MIC values are reported as the median of three independent determinations.

## Drug combination assay

The Checkerboard assay was performed to determine the possible synergistic interactions between the chosen EPI-FP and the INH and RMP. The culture suspension was prepared as described in the above section. The culture control, in the form of an untreated bacterial suspension, was maintained to verify the viability of the growth conditions. FP, INH, and RMP were twofold serially diluted in 7H9 broth from their respective MICs in a 96-well microtiter plate such that each well had a unique combination of FP and drug concentrations. The plates were incubated at 37 °C for 5 days and microscopically examined for the presence of cord formation, which is a measure of *M. tuberculosis* growth. To quantify the synergistic inhibitory effect of FP in combination

with RMP and INH, the fractional inhibitory concentration (FIC) and the modulation factor (MF) were calculated on the basis of the MIC values (Amaral et al. 2020).

## Cloning and overexpression of Rv0933 and Rv0194

### Mycobacterial transformation and expression of recombinant protein

The expression of *Rv0933* and *Rv0194* genes was carried out as described previously (Nirmal et al. 2023b). In brief, the genes encoding Rv0933 and Rv0194 were cloned into the pMV261 vector and transformed into the *Escherichia coli* DH5α strain. The recombinant strains were screened by plating on LB agar plates supplemented with 35 µg/mL kanamycin. The *Rv0933*-pMV261 and *Rv0194*-pMV261 plasmids were isolated from the recombinant strains via a Qiagen miniprep kit (Cat. No. 27104), and 200 to 400 ng of each plasmid was transformed into *Mycobacterium smegmatis* $mc^2$−155 competent cells through electroporation. The transformation was confirmed through PCR using gene-specific primers. The recombinant *M. smegmatis* cultures were incubated for 48 h at 37 °C until they reached an optical density of 0.6 at 600 nm ($OD_{600}$) for further studies.

### Analysis of the transcriptional levels of Rv0933 and Rv0194 in recombinant strains of *M. smegmatis*

The transformants were confirmed via gene-specific PCR. The recombinant *M. smegmatis* were cultured in Middlebrook 7H9 broth and exposed to first-line anti-TB drugs at 37 °C for 48 h to induce gene expression. Cultures without drug exposure were kept as controls under identical incubation conditions. Total RNA was extracted via the RNeasy Mini Kit (Qiagen GmbH), and complementary DNA (cDNA) synthesis was performed via the First Strand cDNA Synthesis Kit (Thermo Fischer Scientific, Inc.). Gene expression was assessed via quantitative real-time polymerase chain reaction (qRT−PCR) with the PrimeScript One-Step RT−PCR Kit (TakaraBio). The 16S housekeeping gene was used as an internal control.

## Cytotoxicity testing

The cytotoxicity of the identified efflux pump inhibitors was assessed in peripheral blood mononuclear cells (PBMCs) and THP-1 cells via a trypan blue exclusion assay. Commercially obtained PBMCs (HiMedia) at a density of $3.92 \times 10^5$ cells/mL and THP-1 cells at $1 \times 10^5$ cells/mL were treated with the selected compounds at four different concentrations: 3X, 2X, 1X, and 0.5X of their MIC, corresponding to 1000 µg/mL, 500 µg/mL, 250 µg/mL, and 125 µg/mL, respectively. Untreated cells were used as controls. The experiment was conducted in triplicate, and the cells were cultured in RPMI-1640 medium supplemented with 10% foetal bovine serum at 37 °C and 5% $CO_2$ for 72 h. After incubation, the cells were mixed at a 1:4 ratio with 0.4% trypan blue (HiMedia), and viable cells were counted via a Rosenthal counting chamber under an inverted microscope. The percentage of cell viability was calculated via the following formula:

$$\text{Percentage of Viability} = \left\{ \frac{(\text{Number of viable cells in the test})}{\text{Number of viable cells in the untreated control}} \right\} \times 100$$

# Results

## In silico screening of EPIs against Rv0933 and Rv0194

Ramachandran plots generated by the PDBsum server for the predicted protein structures revealed that most residues were positioned in core regions, indicating an absence of steric hindrance and suggesting high stereochemical quality (Fig. 1). This was further supported by PROCHECK analysis, which confirmed that both the overall and residue-by-residue geometries of the models were within acceptable ranges. The presence of residues in allowed regions indicated plausible conformations, with slightly shorter van der Waals radii. Only a few residues were found in disallowed regions (white areas), implying that the predicted models had few sterically unfavourable conformations. Overall, these findings support the reliability and accuracy of the predicted protein structures. Lead compounds were selected from the ZINC database via multiple criteria, including the Glide score, Glide energy, ligand−protein interaction energy, hydrophobic interactions, hydrogen bonding, internal energy, π−π stacking interactions, root mean square deviation (RMSD), and desolvation energy. The compounds identified by AutoDock Vina through molecular docking were then consolidated, and post-docking validation was performed. The top ten compounds, ranked by the Glide score, were shortlisted (Table 1). These compounds were further evaluated for their docking scores with efflux membrane proteins and tested for MICs via the micro broth dilution method.

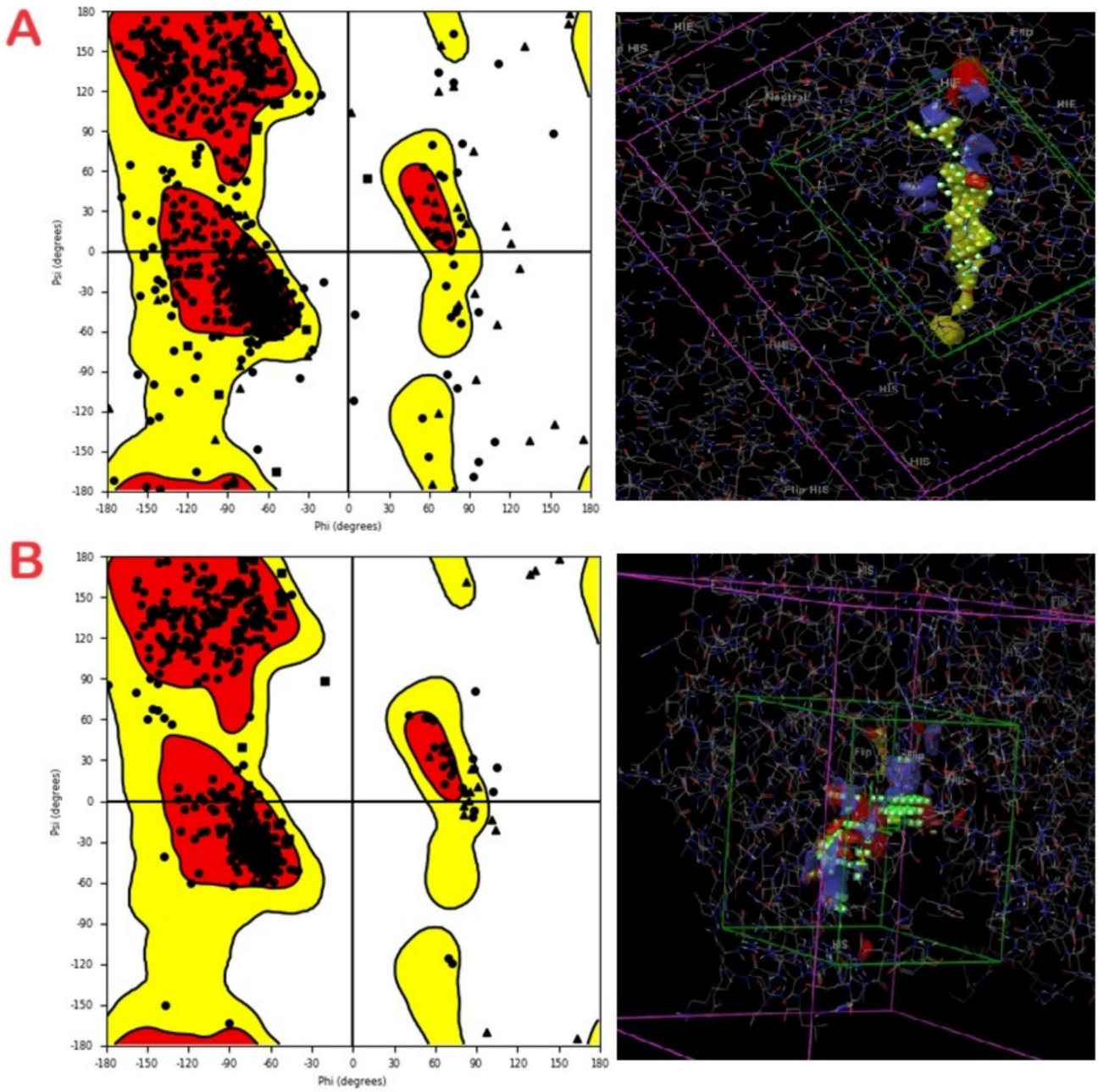


**Fig. 1** Structural validation and molecular docking visualization of the *M. tuberculosis* efflux proteins Rv0194 (**A**) and Rv0933 (**B**). The left panels show Ramachandran plots confirming the good stereochemical quality of the modelled efflux proteins. The right panels depict ligand docking within the active sites, highlighting interactions in the binding pockets

## Drug likeness analysis for shortlisted efflux inhibitors against Rv0194c

The seven selected compounds were subjected to drug-likeness screening, which evaluated parameters such as molecular weight, hydrogen bond donors, hydrogen bond acceptors, log P (octanol/water partition coefficient), log P Caco (cell permeability), log Kp (skin permeability), and human oral absorption, along with their compliance with Lipinski's rule of five (Table 2). The drug-likeness of the selected compounds was evaluated on the basis of key physicochemical properties, including molecular weight, lipophilicity (MLogP), hydrogen bond donors, and hydrogen bond acceptors, following Lipinski's rule of five. Five out of six compounds—trichlorocarbinalide (TCC), thalidomide (Th), lenalidomide (LN), levomefolic acid (LFA), and flurbiprofen (FP)—had molecular weights below the recommended threshold of 500 g/mol, with iohexol (IHX) being

**Table 1** E-pharmacophore modelling of the top ten small-molecule inhibitors targeting the multidrug efflux pumps Rv0933 and Rv0194 associated with INH and RMP resistance in *M. tuberculosis*

| Compounds screened for Rv0933 & Rv0194 | Compound 2D structure | Zinc ID | Docking score |
|---|---|---|---|
| flurbiprofen | 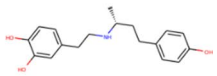 | ZINC000000000323 | -7.9 |
| iohexol | 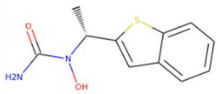 | ZINC000003830944 | -6.75 |
| fluvastatin | 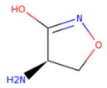 | ZINC000001530639 | -6.25 |
| trichlorocarbinalide | 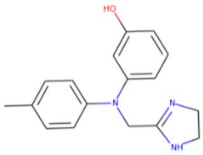 | ZINC000000020251 | -6.28 |
| thalidomide | 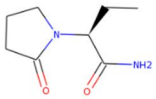 | ZINC000000968303 | -7.21 |
| conivaptan | 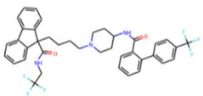 | ZINC000012503187 | -6.35 |
| almotriptan | 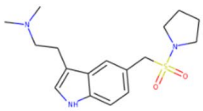 | ZINC000000018087 | -6.32 |
| lomitapide | 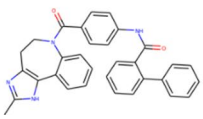 | ZINC000027990463 | -6.30 |

**Table 2** Drug-likeness screening of selected compounds based on key physicochemical properties

| Compounds | Molecular weight (g/mol) | Lipophilicity (MLog*P*) | Hydrogen bond donors | Hydrogen bond acceptors |
|---|---|---|---|---|
| | **< 500** | **< 5** | **< 5** | **< 10** |
| Iohexol | 821.13 | 2 | 1 | 2 |
| Trichlorocarbinalide | 315.58 | 2 | 2 | 2 |
| Thalidomide | 258.23 | 1 | 1 | 2 |
| Lenalidomide | 259.26 | 2 | 2 | 4 |
| Levomefolic acid | 459.5 | 2 | 8 | 4 |
| Flurbiprofen | 244.26 | 1 | 1 | 1 |

the only exception, exceeding this limit at 821.13 g/mol. All the compounds exhibited acceptable lipophilicities, with MLogP values less than 5. Additionally, all the compounds complied with the criterion of fewer than 5 hydrogen bond donors. With respect to hydrogen bond acceptors, all but LFAs (8 acceptors) remained below the limit of 5, although LFAs still fell within the broader allowance of fewer than 10 acceptors. These findings suggest that most of the compounds, particularly TCC, Th, LN, and FP, possess favourable drug-like properties, indicating their potential as viable candidates for further development as EPIs.

## Rifampicin and isoniazid exposure increase the expression of Rv0933 and Rv0194 in *M. smegmatis*

The presence of Rv0933 and Rv0194 in rMSM was confirmed via PCR (Supplementary Fig. 1). The screened rMSM were exposed to RMP and INH at 37 °C for 48 h before RNA extraction. Unexposed cultures were used as controls. The overexpression of Rv0933 and Rv0194 in the presence of RMP and INH was observed in the recombinant *M. smegmatis* strains in which the corresponding genes were cloned. The fold change in Rv0933 and Rv0194 gene expression was calculated by normalizing the expression values of the internal housekeeping genes to those of the recombinant strains not exposed to RMP or INH. The presence of RMP at a suboptimal level markedly increased the expression of Rv0933 sevenfold. The expression of Rv0194 increased 0.3-fold in the presence of INH (Fig. 2).

## MIC determination and synergistic anti-TB activity of the lead compounds against MDR-TB isolates

The shortlisted lead compounds, IHX, TCC, FP (2-fluoro-α-methyl-4-biphenylacetic acid), LN, LFA, and Th, were procured and assessed for their anti-TB activity by determining their MICs against *M. tuberculosis* H37Rv and MDR strains of *M. tuberculosis* ($n = 10$). FP presented the lowest MIC values among the tested compounds, indicating greater potency against the MDR-TB isolates (Table 3).

**Table 3** MICs of three shortlisted lead compounds against ten MDR-TB isolates

| Culture No | Minimum inhibitory concentration (MIC) | | | | |
|---|---|---|---|---|---|
| | INH (μg/mL) | RMP (μg/mL) | IHX (μg/mL) | TCC (μg/mL) | FP (μg/mL) |
| MDR01 | 1 | > 16 | > 1000 | 500 | > 1000 |
| MDR02 | 4 | > 16 | > 1000 | 1000 | 1000 |
| MDR03 | 4 | > 16 | > 1000 | > 1000 | 500 |
| MDR04 | 4 | > 16 | > 1000 | 500 | > 1000 |
| MDR05 | > 4 | > 16 | > 1000 | 1000 | 1000 |
| MDR06 | 4 | > 16 | 1000 | 500 | 250 |
| MDR07 | 2 | > 16 | > 1000 | > 1000 | 250 |
| MDR08 | 4 | > 16 | 1000 | 500 | 250 |
| MDR09 | 2 | > 16 | > 1000 | 500 | > 1000 |
| MDR10 | > 4 | > 16 | 1000 | 250 | 250 |

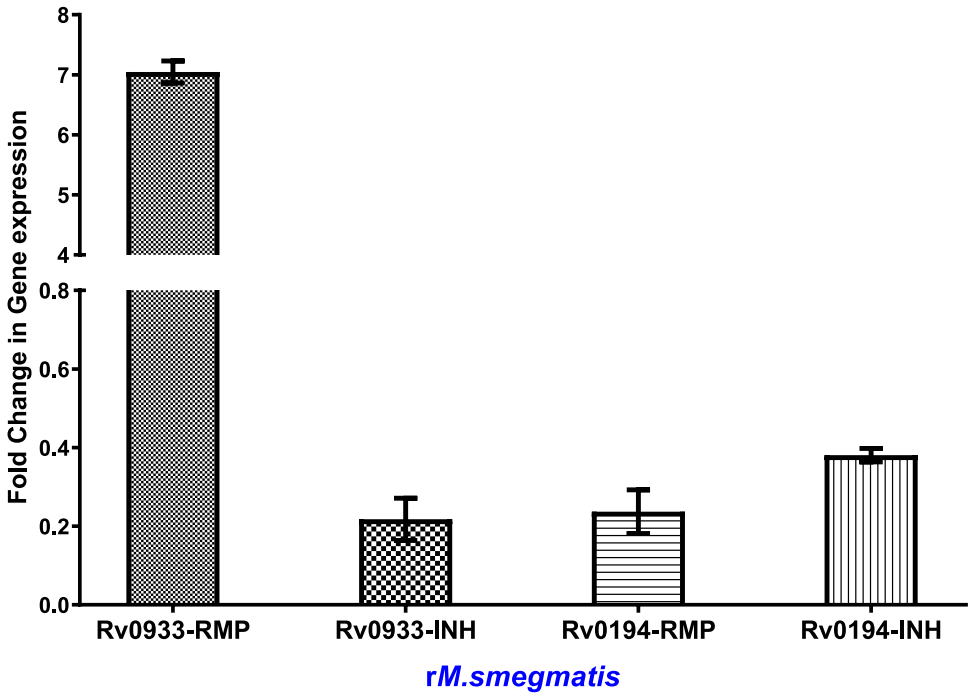


**Fig. 2** Fold change in the gene expression of the *M. tuberculosis* efflux pump genes Rv0933 and Rv0194 in recombinant *M. smegmatis* under drug-induced conditions (RMP and INH). Gene expression was normalized to that of untreated controls

**Table 4** In vitro RMP and INH efflux inhibitor combination studies showing synergistic effects of FP with RMP and INH

| MDR-TB clinical isolates | MIC of FP (µg/mL) | | | MIC of RMP (µg/mL) | | FIC of RMP + FP | MF of RMP + FP | MIC of INH (µg/mL) | | FIC of INH + FP | MF of INH + FP |
|---|---|---|---|---|---|---|---|---|---|---|---|
| | Without drug (µg/mL) | With RMP (µg/mL) | With INH (µg/mL) | Without FP (µg/mL) | With FP (µg/mL) | | | Without FP (µg/mL) | With FP (µg/mL) | | |
| MDR 06 | 250 | 125 | 31.25 | > 16 | 1 | 0.0625 | 16 | 4 | 0.5 | 0.125 | 8 |
| MDR 08 | 250 | 62.5 | 7.8 | > 16 | 0.5 | 0.0312 | 32 | 4 | 0.015 | 0.003 | 266 |

**Table 5** In vitro RMP and INH efflux inhibitor combination studies showing the synergistic effects of TCC with RMP and INH

| MDR-TB clinical isolates | MIC of TCC (µg/mL) | | | MIC of RMP (µg/mL) | | FIC of RMP + TCC | MF of RMP + TCC | MIC of INH (µg/mL) | | FIC of INH + TCC | MF of INH + TCC |
|---|---|---|---|---|---|---|---|---|---|---|---|
| | Without drug (µg/mL) | With RMP (µg/mL) | With INH (µg/mL) | Without TCC (µg/mL) | With TCC (µg/mL) | | | Without TCC (µg/mL) | With TCC (µg/mL) | | |
| MDR 06 | 500 | 250 | 62.5 | > 16 | 2 | 0.125 | 8 | 4 | 0.5 | 0.125 | 8 |
| MDR 08 | 250 | 32.5 | 15.62 | 16 | 0.5 | 0.03125 | 32 | 4 | 0.25 | 0.0625 | 16 |

Two isolates were selected for a combination assay via the Checkerboard method. TCC and FP were tested with INH and RMP. Both FP and TCC showed synergistic activity, as evidenced by both the FIC and MF values (Tables 4 & 5).

### Cytotoxicity testing of peripheral blood mononuclear cells

The calculated $LD_{50}$ values for the PBMCs were 680.48 µg/mL (FP) and 693.77 µg/mL (trichlorocarbanilide), indicating relatively lower cytotoxicity. In contrast, the THP-1 cells treated with the same agent presented a much steeper decline in viability, suggesting a greater cytotoxic effect. The $LD_{50}$ values for THP-1 cells were significantly lower at 39.04 µg/mL (FP) and 43.54 µg/mL (trichlorocarbanilide), indicating a stronger toxic effect on these cells.

## Discussion

TB continues to pose a significant global health challenge, with an estimated 2 million deaths annually attributed to this infectious disease. The emergence and rapid dissemination of MDR and XDR *M. tuberculosis* strains have severely constrained the efficacy of conventional first-line anti-TB therapeutic regimens, necessitating the urgent exploration of novel treatment strategies. Among the mechanisms conferring resistance in mycobacteria, reduced cell wall permeability and active drug efflux mediated by EPs play crucial roles in limiting intracellular drug accumulation, thereby diminishing antimicrobial efficacy. Although various EPs, such as Rv0194 and Rv0933, have been annotated within the *M. tuberculosis* genome, comprehensive functional characterization remains inadequate (Lin et al. 2021). Previous studies have demonstrated that the overexpression of Rv0194 in *Mycobacterium smegmatis* significantly decreases the intracellular accumulation of ethidium bromide and contributes to broad-spectrum multidrug resistance by increasing the MICs of multiple antibiotics (Danilchanka et al. 2008). We also observed increased expression of these EPs in the presence of first-line anti-TB drugs such as RMP and INH (Fig. 2), highlighting their importance in conferring resistance to RMP and INH. In comparison, Rv0933 expression was high in the presence of RMP, whereas Rv0194 expression was high in the presence of INH. On the basis of these findings, our study aimed to identify and characterize potential EPIs derived from FDA-approved compounds via a combination of virtual screening and in vitro evaluation.

Through virtual screening, six candidate EPIs were shortlisted on the basis of their binding affinities with Rv0933 and Rv0194. These compounds were subsequently subjected to experimental validation against a panel of ten MDR-TB clinical isolates and the reference *M. tuberculosis* H37Rv strain via the micro broth dilution method. The MICs of RMP and INH were also estimated similarly. The MDR strains exhibited high levels of resistance to RMP (> 16 µg/mL) and INH (> 4 µg/mL), which is consistent with previous reports on resistant clinical isolates. Among the six shortlisted compounds, two molecules, namely, TCC and FP, demonstrated intrinsic anti-TB activity against these MDR-TB strains, albeit at relatively high concentrations. Given their observed inhibitory effects, these compounds were further assessed for their potential synergistic interactions with RMP and INH via the FIC and MF indices.

FP is a well-established non-steroidal anti-inflammatory drug (NSAID) belonging to the arylpropionic acid class, which also includes widely used medications such as ibuprofen. As an FDA-approved drug for the treatment of rheumatoid arthritis, its pharmacokinetic and safety profiles are well documented, facilitating potential drug repurposing efforts (Valentovic 2007). Although previous studies have explored its anti-TB activity, FP was not pursued further because of its relatively high MIC (> 90 mg/L) (Guzman et al. 2013). However, in our study, we demonstrated that FP exhibits intrinsic anti-TB activity at elevated concentrations in MDR-TB strains and exerts a potent synergistic effect when combined with RMP and INH, effectively reducing their MICs to clinically relevant levels. Additionally, the known anti-inflammatory properties of FPs may provide host-directed benefits by mitigating the excessive immune response and tissue pathology, such as inflammation associated with TB progression (Ivanov et al. 2024).

TCC, also known as triclocarban, is a well-characterized antibacterial agent that disrupts lipid metabolism in bacteria, fungi, and plants, ultimately inhibiting cell membrane synthesis and thereby preventing cell growth. Although its widespread use in consumer products has led to regulatory restrictions, its application as a therapeutic agent remains an area of active investigation (Iacopetta et al. 2021). While its direct anti-TB activity has not been extensively characterized, our findings indicate that TCC exerts synergistic effects against MDR-TB strains in the presence of either RMP or INH (Tables 4 & 5).

The results of the in vitro experiments indicated that FP and TCC synergistically interact with both RMP and INH, significantly reducing their MIC values to the critical concentration required to inhibit drug-sensitive *M. tuberculosis* strains. The MDR-TB strains, which originally exhibited resistance to RMP (> 16 µg/mL) and INH (> 4 µg/mL), demonstrated marked susceptibility when cotreated with FP, with MIC reductions to 1 µg/mL for RMP and 0.5–0.015 µg/mL for INH (Table 4). An FIC index value of < 0.5 indicates synergy, 0.5–4 indicates indifference, and > 4 indicates antagonism. Similarly, the MF is also above 4. The results showed that FPs

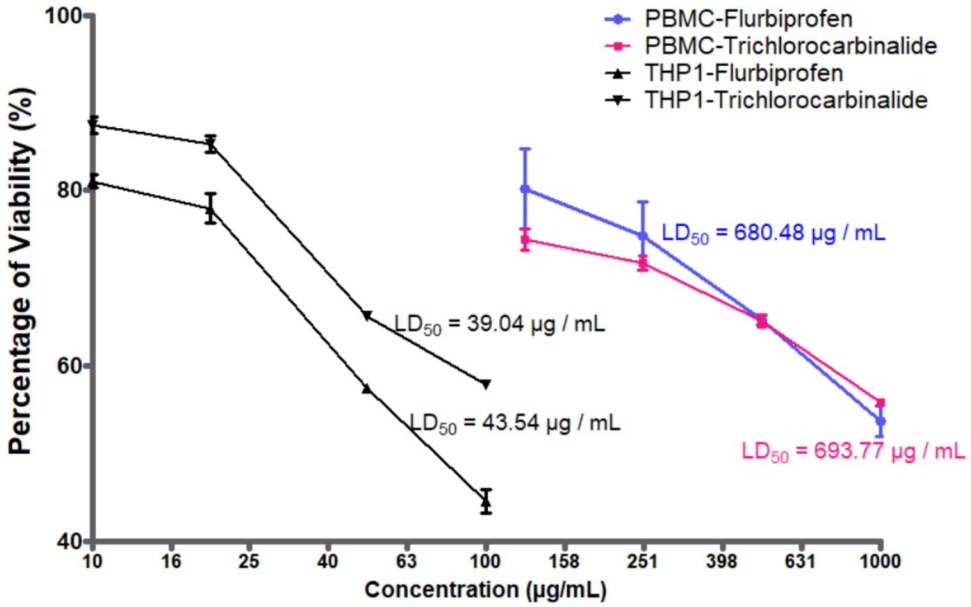


**Fig. 3** Dose-dependent cytotoxicity of FP and TCC in human PBMCs and THP-1 cells. $LD_{50}$ values (concentrations causing 50% loss of viability) are indicated for each treatment group. The data represent the means ± SDs of triplicate experiments

combined with INH and RMP had synergistic effects on both isolates (Tables 4 & 5). This highlights the potential for combination therapy in MDR-TB treatment. The synergistic activity of FP and TCC suggests their potential for repurposing as adjunctive therapies in combination with first-line anti-TB drugs, such as RMP and INH. As previously discussed, these EPs exhibited differential expression in response to RMP and INH; however, both EPs were effectively inhibited by FP and TCC. From a translational perspective, this finding is significant, as it suggests a potential reduction in pill burden.

Given the necessity of assessing the cytotoxicity of potential therapeutic agents, we evaluated the impact of TCC and FP on PBMCs and THP-1 cells. PBMCs were selected as a representative model of primary human immune cells, whereas THP-1 cells, derived from an acute monocytic leukaemia cell line, served as a model for macrophage-like cells. Both compounds demonstrated favourable safety profiles in PBMCs, as evidenced by their high $LD_{50}$ values. However, these compounds exhibited significant cytotoxicity toward THP-1 cells, with substantially lower $LD_{50}$ values (Fig. 3). This differential cytotoxicity could be attributed to the oncogenic nature of THP-1 cells, as previous studies have reported that cancerous cells often exhibit heightened sensitivity to specific compounds. Notably, FPs and their derivatives were previously recognized for their anticancer activity against lung and breast cancer, suggesting a potential dual role in antimicrobial and anticancer therapeutics with COX inhibition potential (Caban-Toktas et al. 2020; Sonam et al. 2025). Similarly, TCC shares structural similarities with β-carbolines, which have been reported to exert anticancer effects through DNA intercalation mechanisms (Soni et al. 2021).

Our study highlights the potential of FP and TCC as efflux pump inhibitors with activity against MDR *M. tuberculosis* strains. The synergistic interaction between FP and TCC with first-line anti-TB drugs underscores its promise as a repurposed adjunctive therapy for drug-resistant TB. However, given the limited number of MDR-TB strains analyzed in this study, further validation with a larger cohort of clinical isolates is necessary to confirm these findings to facilitate their translation into clinical applications for combating drug-resistant TB.

## Conclusion

Our study underscores the critical role of efflux pump inhibitors in addressing drug-resistant *M. tuberculosis*. By targeting key resistance mechanisms involving Rv0194 and Rv0933, we identified TCC and FP as promising candidates. These compounds demonstrated antimycobacterial activity against MDR strains, with FPs exhibiting significant synergy with RMP and INH, effectively lowering their MIC values. Additionally, both inhibitors displayed favourable cytotoxicity profiles in PBMCs, supporting their potential for further development as adjunctive therapies. Future research should optimize these compounds, explore structural analogues, and conduct comprehensive in vivo efficacy and safety studies to facilitate their clinical translation in combating drug-resistant TB.

**Supplementary information** The online version contains supplementary material available at https://doi.org/10.1007/s12223-025-01319-8.

**Author contribution** CRN, PE, and AD conceptualized and designed the study. AD and PE received financial support from ICMR for this research work. PE and RD performed the TB culture retrieval, in vitro assay, and clinical validation. PE and NB performed the bioinformatic screening and validation. PE, CRN, SER, and AD analysed the data. CRN, PE, and SER wrote the manuscript. AD proofread the manuscript. All the authors have read and approved the final manuscript.

**Funding** The authors are thankful for the financial support provided by the Indian Council of Medical Research (ICMR). PE received an ICMR-RA fellowship (No. Fellowship/TB/40/2020–7030). PE and AD received an intramural grant from ICMR-NIRT to meet the consumable cost (Fellowship/Bact/RA/Padmasini/31.10.2022). CRN received an ICMR-RA fellowship (No. Fellowship/2020–6327/RA). SER received ICMR-PDF (F.No. 3/1/3/PDF (16)/- 2019-HRD 3).

**Data Availability** All data of this study have been presented in the manuscript.

## Declarations

**Ethical approval** This study was approved by the Institutional Ethics Committee of the ICMR-National Institute for Research in Tuberculosis (NIRT, Chennai) before its implementation (No: 021/NIRT-IEC/2021; dtd 25/2/2021).

This study was also submitted and issued approval from the institutional bioethics committee for Category III as per the guidelines of DBT held at ICMR NIRT, Chennai, on 06/10/2021.

**Conflict of interest** The authors declare no competing interests.

## References

Amaral RCRd, Caleffi-Ferracioli KR, Demitto FdO et al (2020) Is the efflux pump inhibitor Verapamil a potential booster for isoniazid against *Mycobacterium tuberculosis*? Braz J Pharm Sci 56. https://doi.org/10.1590/s2175-97902020000218309

Biswas SS, Roy JD (2024) Prediction of structure of mycobacterial efflux pump protein Rv0194 and molecular dynamics simulation of the predicted structures. Biocatal Agric Biotechnol 61:103381. https://doi.org/10.1016/j.bcab.2024.103381

Caban-Toktas S, Sahin A, Lule S et al (2020) Combination of paclitaxel and R-flurbiprofen loaded PLGA nanoparticles suppresses glioblastoma growth on systemic administration. Int J Pharm 578:119076. https://doi.org/10.1016/j.ijpharm.2020.119076

Danilchanka O, Mailaender C, Niederweis M (2008) Identification of a novel multidrug efflux pump of *Mycobacterium tuberculosis*. Antimicrob Agents Chemother 52:2503–2511. https://doi.org/10.1128/AAC.00298-08

Davies GR, Aston S (2023) Update on drug treatments for multidrug resistant tuberculosis. Curr Opin Infect Dis 36:132–139. https://doi.org/10.1097/QCO.0000000000000899

De Pires V, Blundell TL, Ascher DB (2015) pkCSM: predicting small-molecule pharmacokinetic and toxicity properties using graph-based signatures. J Med Chem 58:4066–4072. https://doi.org/10.1021/acs.jmedchem.5b00104

de Souza JVP, Murase LS, Caleffi-Ferracioli KR et al (2020) Isoniazid and verapamil modulatory activity and efflux pump gene expression in *Mycobacterium tuberculosis*. Int J Tuberc Lung Dis 24:591–596. https://doi.org/10.5588/ijtld.19.0458

Duffey M, Jumde RP, da Costa RMA et al (2024) Extending the potency and lifespan of antibiotics: inhibitors of gram-negative bacterial efflux pumps. ACS Infect Dis 10:1458–1482. https://doi.org/10.1021/acsinfecdis.4c00091

Guan L (2022) Structure and mechanism of membrane transporters. Sci Rep 12:13248. https://doi.org/10.1038/s41598-022-17524-1

Guzman JD, Evangelopoulos D, Gupta A et al (2013) Antitubercular specific activity of ibuprofen and the other 2-arylpropanoic acids using the HT-SPOTi whole-cell phenotypic assay. BMJ Open 3:e002672. https://doi.org/10.1136/bmjopen-2013-002672

Iacopetta D, Catalano A, Ceramella J et al (2021) The different facets of triclocarban: a review. Molecules 26:2811. https://doi.org/10.3390/molecules26092811

Irwin JJ, Shoichet BK (2005) ZINC–a free database of commercially available compounds for virtual screening. J Chem Inf Model 45:177–182. https://doi.org/10.1021/ci049714+

Ivanov I, Manolov S, Bojilov D et al (2024) Novel flurbiprofen derivatives as antioxidant and anti-inflammatory agents: synthesis, *in silico*, and *in vitro* biological evaluation. Molecules 29:385. https://doi.org/10.3390/molecules29020385

Kollman PA, Massova I, Reyes C et al (2000) Calculating structures and free energies of complex molecules: combining molecular mechanics and continuum models. Acc Chem Res 33:889–897. https://doi.org/10.1021/ar000033j

Li G, Zhang J, Guo Q et al (2015) Study of efflux pump gene expression in rifampicin-monoresistant *Mycobacterium tuberculosis* clinical isolates. J Antibiot (Tokyo) 68:431–435. https://doi.org/10.1038/ja.2015.9

Lin Y, Dong Y, Gao Y et al (2021) Identification of CTL epitopes on efflux pumps of the ATP-binding cassette and the major facilitator superfamily of *Mycobacterium tuberculosis*. J Immunol Res 2021:1–13. https://doi.org/10.1155/2021/8899674

Lipinski CA, Lombardo F, Dominy BW, Feeney PJ (2001) Experimental and computational approaches to estimate solubility and permeability in drug discovery and development settings. Adv Drug Deliv Rev 46:3–26. https://doi.org/10.1016/S0169-409X(00)00129-0

Long Y, Wang B, Xie T et al (2024) Overexpression of efflux pump genes is one of the mechanisms causing drug resistance in *Mycobacterium tuberculosis*. Microbiol Spectr 12. https://doi.org/10.1128/spectrum.02510-23

Morris GM, Huey R, Lindstrom W et al (2009) AutoDock4 and AutoDockTools4: automated docking with selective receptor flexibility. J Comput Chem 30:2785–2791. https://doi.org/10.1002/jcc.21256

Nirmal CR, Rajadas SE, Balasubramanian M et al (2023) Dodecanoic acid & palmitic acid disarms rifampicin resistance by putatively targeting mycobacterial efflux pump Rv1218c. Indian J Med Res 157:192–203. https://doi.org/10.4103/ijmr.ijmr_1610_22

Nirmal CR, Rajadas SE, Balasubramanian M et al (2023) Myoinositol and methyl stearate increases rifampicin susceptibility among drug-resistant *Mycobacterium tuberculosis* expressing Rv1819c. Chem Biol Drug des 101:883–895. https://doi.org/10.1111/cbdd.14197

Pule CM, Sampson SL, Warren RM et al (2016) Efflux pump inhibitors: targeting mycobacterial efflux systems to enhance TB therapy. J Antimicrob Chemother 71:17–26. https://doi.org/10.1093/jac/dkv316

Remm S, Earp JC, Dick T et al (2022) Critical discussion on drug efflux in Mycobacterium tuberculosis. FEMS Microbiol Rev 46:fuab050. https://doi.org/10.1093/femsre/fuab050

Shelley JC, Cholleti A, Frye LL et al (2007) Epik: a software program for pK a prediction and protonation state generation for drug-like

molecules. J Comput Aided Mol des 21:681–691. https://doi.org/10.1007/s10822-007-9133-z
Sonam S, Jelača S, Laube M et al (2025) Carborane conjugates with ibuprofen, fenoprofen and flurbiprofen: synthesis, characterization, COX inhibition potential and in vitro activity. Chem Med Chem 20:e202400018. https://doi.org/10.1002/cmdc.202400018
Soni JP, Yeole Y, Shankaraiah N (2021) β-Carboline-based molecular hybrids as anticancer agents: a brief sketch. RSC Med Chem 12:730–750. https://doi.org/10.1039/D0MD00422G
Valentovic M (2007) Flurbiprofen. In: Enna S J, Bylund DB (eds) xPharm: The Comprehensive Pharmacology Reference. Elsevier, pp 1–6. https://doi.org/10.1016/B978-008055232-3.61777-5
Valıyeva G, Durupınar B, Coban AY (2023) Efflux pump effects on *Mycobacterium tuberculosis* drug resistance. J Chemother 35:601–609. https://doi.org/10.1080/1120009X.2023.2173857
Global Tuberculosis Programme (2023) Global tuberculosis report - 2023. World Health Organization, Geneva
Zhang Y (2008) I-TASSER server for protein 3D structure prediction. BMC Bioinformatics 9:40. https://doi.org/10.1186/1471-2105-9-40